

Perfluorobutane contrast-enhanced ultrasonography: a new standard for ultrasonography-guided thermal ablation of sonographically occult liver tumours?

Haiyuan Shi¹, MBBS, FRCR, Yi-Ting Ong², PhD, Apoorva Gogna³, MBBS, FRCR, Nanda Venkatanarasimha³, MBBS, FRCR, Sarat Kumar Sanamandra³, MBBS, FRCR, Sum Leong³, MBChB, FFRRCSI, Farah Gillan Irani³, MBBS, FRCR, Richard Hoau Gong Lo³, MBBS, FRCR, Chow Wei Too³, MBBS, FRCR

INTRODUCTION Image-guided thermal ablation, preferably with ultrasonography (US), is increasingly used for treatment of small liver tumours. Perfluorobutane-contrast-enhanced US (pCEUS) is a promising tool that may allow for targeting of tumours that are otherwise imperceptible on greyscale US. Although pCEUS has been reported to be effective, the literature has been limited outside of Japan and South Korea. We aimed to provide data that supports the use of pCEUS in the thermal ablation of sonographically occult liver tumours.

METHODS We conducted a retrospective single-centre study of 35 consecutive patients who underwent pCEUS-guided ablation of 48 liver tumours with a median size of 1.2 cm. Peri-procedural, one-month post-treatment and relevant follow-up imaging studies were reviewed. Electronic records were also obtained, with long-term follow-up data of 12–28 months being available for 32 patients.

RESULTS 36 (75%) tumours that were imperceptible on greyscale US became visible with pCEUS. Overall, complete tumour ablation at one month was 89%. 1 (3%) patient developed a major complication following treatment, while 6 (17%) had minor post-treatment complaints. The local tumour progression rate was 17%, with a median time of 14 months.

CONCLUSION pCEUS has a role in US-guided thermal ablation of liver tumours, offering a high technical success rate that is comparable to reported data. Additional benefits may include improved procedural time and freedom from ionising radiation.

Keywords: contrast-enhanced ultrasonography, hepatocellular carcinoma, liver tumour, perfluorobutane, thermal ablation

INTRODUCTION

Small liver tumours are increasingly being treated with image-guided thermal ablation, also known as radiofrequency ablation (RFA) or microwave ablation (MWA).^(1–3) In our practice, ultrasonography (US) is preferred for tumour localisation and ablation guidance. There are several advantages to US: (a) real-time high-resolution imaging to compensate for constant respiratory movements of the liver; (b) high manoeuvrability, which facilitates rapid change of imaging planes, as is required to avoid important structures during needle advancement; and (c) the lack of radiation to both the patient and the operator. Unfortunately, tumours are not always readily identifiable on conventional greyscale US, prompting the operator to adopt alternative techniques, most commonly computed tomography (CT) fluoroscopic guidance, sometimes using anatomical landmarks if the lesion of interest is imperceptible on non-contrast CT.

Many sonographically occult tumours can be rendered visible with administration of US contrast agents. Commonly used ‘blood pool’ agents, such as sulfur hexafluoride microbubbles (SonoVue®, Bracco Imaging, Milan, Italy), allow for intense but fleeting arterial enhancement of tumours.⁽⁴⁾ However, given the short operating window, they are not ideal for lesion targeting. A newer contrast agent comprising perfluorobutane microspheres, Sonazoid® (Daiichi Sankyo, Tokyo, Japan), was first introduced

in 2007 and offers an additional Kupffer phase (Fig. 1). Active phagocytosis of contrast microspheres by hepatic Kupffer cells leads to enhancement of normal liver parenchyma.^(5–7) Tumours, deficient in Kupffer cells, are made visible as discreet hypoechoic ‘defects’. As such, the mode of action of perfluorobutane-contrast-enhanced US (pCEUS) is comparable to the widely-used magnetic resonance (MR) imaging with liver-specific contrast (e.g. gadolinium ethoxybenzyl diethylenetriamine pentaacetic acid [i.e. Gd-EOB-DTPA or Primovist®]), as they both localise to normal liver tissue with tumours seen as ‘black holes’ against a bright background. As a diagnostic tool, pCEUS use is supported by the Asian Pacific Association for the Study of the Liver and has a sensitivity comparable to that of dynamic CT and MR imaging.⁽⁸⁾

To the interventionist, pCEUS is a viable method for lesion targeting because its unique Kupffer phase lasts up to 60 minutes. However, reports of its use for liver tumour ablation have been relatively limited outside of Japan and South Korea, probably owing to its less widespread availability and comparatively recent introduction. Through this study, we aimed to provide additional data in support of pCEUS as a preferred tool for image-guided ablation of liver tumours that are imperceptible on greyscale US.

METHODS

Institutional review board approval (ref no. 2016/2745) was obtained for this retrospective single-centre analysis. Between

¹Department of Diagnostic Radiology, Changi General Hospital, ²Duke-NUS Medical School, ³Department of Vascular and Interventional Radiology, Singapore General Hospital, Singapore

Correspondence: Dr Shi Haiyuan, Associate Consultant, Changi General Hospital, Singapore, 2 Simei Street 3, Singapore 529889. shi.haiyuan@singhealth.com.sg

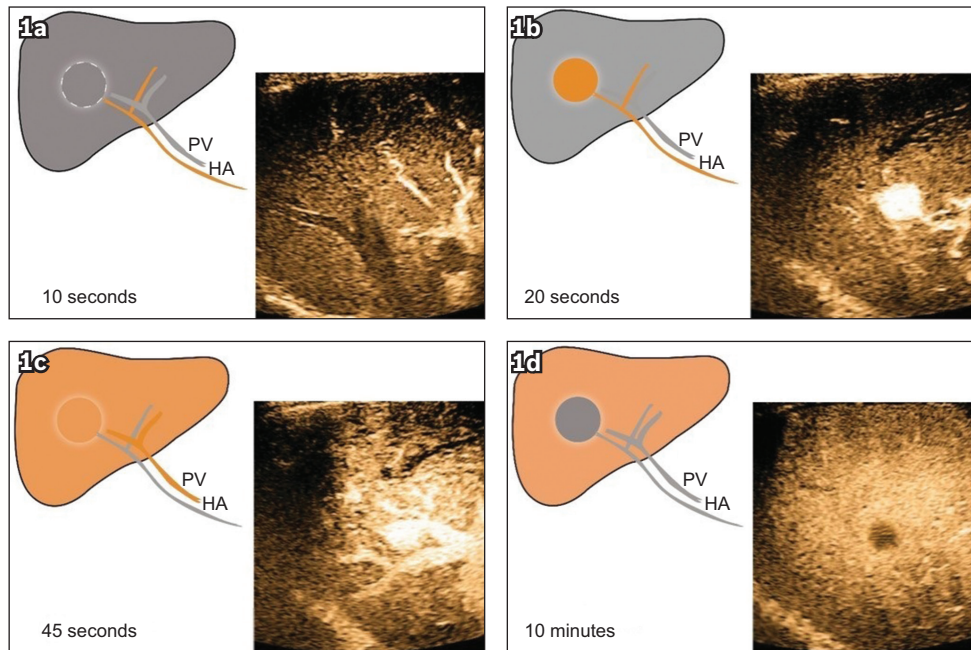


Fig. 1 Dynamic pCEUS images show (a) enhancement of the hepatic arteries at ten seconds; (b) intense enhancement of the tumour at 20 seconds, with demonstration of a prominent arterial feeder; and (c) enhancement of the portal veins, and the liver parenchyma starting to enhance at 45 seconds. The contrast between the liver parenchyma and the tumour is reduced. (d) Dynamic pCEUS image at ten minutes (i.e. the Kupffer phase) shows the normal liver tissue at peak enhancement owing to parenchymal retention of contrast. The tumour demonstrates a 'defect', as it does not have normal Kupffer cells to retain contrast. HA: hepatic artery; pCEUS: perfluorobutane-contrast-enhanced ultrasonography; PV: portal vein

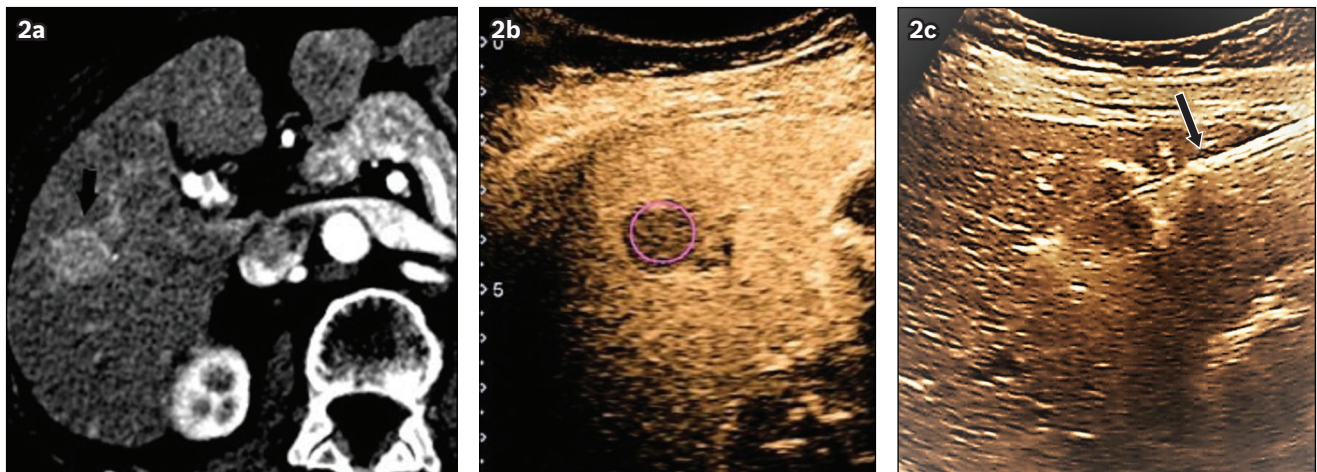


Fig. 2 (a) Initial contrast-enhanced CT image shows enhancing tumour (arrow) during the arterial phase; (b) pCEUS image taken during the delayed Kupffer phase shows a classical Kupffer defect (circle); and (c) pCEUS image taken at about 30 minutes following the initial contrast injection shows the ablation probe (arrow) being placed through the tumour (visualised as the Kupffer defect). pCEUS: perfluorobutane contrast-enhanced ultrasonography

April 2015 and September 2015, 35 consecutive patients underwent pCEUS-guided ablation of 48 hepatic tumours that were imperceptible on greyscale US. Except for one patient who underwent MWA, all treatments were performed with RFA. Close to one-third of the patients had more than one tumour treated at the same setting. The maximum number of ablations per session was three. All treatments were performed by consultant interventional radiologists who were trained in hepatic thermal ablation.

The diagnosis of lesions was based on standard criteria, as follows. For hepatocellular carcinomas (HCCs), American Association for the Study of Liver Diseases criteria were used based on multiphasic CT or liver-specific MR imaging. For metastatic tumours, this was based on the presence of new or

enlarging lesions showing typical signal and enhancement, which were detected on surveillance studies following resection of histologically proven cancers. Treatment was selected following multidisciplinary discussions with managing physicians, surgeons and interventional radiologists. Immediately before the planned treatment, greyscale US was performed by the interventionist for tumour localisation. In cases where the tumour was not visible, pCEUS would follow.

The operator excluded contraindications prior to the administration of US contrast, namely right-to-left shunts, severe pulmonary hypertension and egg allergy.^(9,10) Contrast was prepared by suspending one vial (16 µL) of powdered perfluorobutane microbubbles in a 2-mL vial of solvent (water for injection, included in the packaging). Bolus contrast (0.5 mL) was

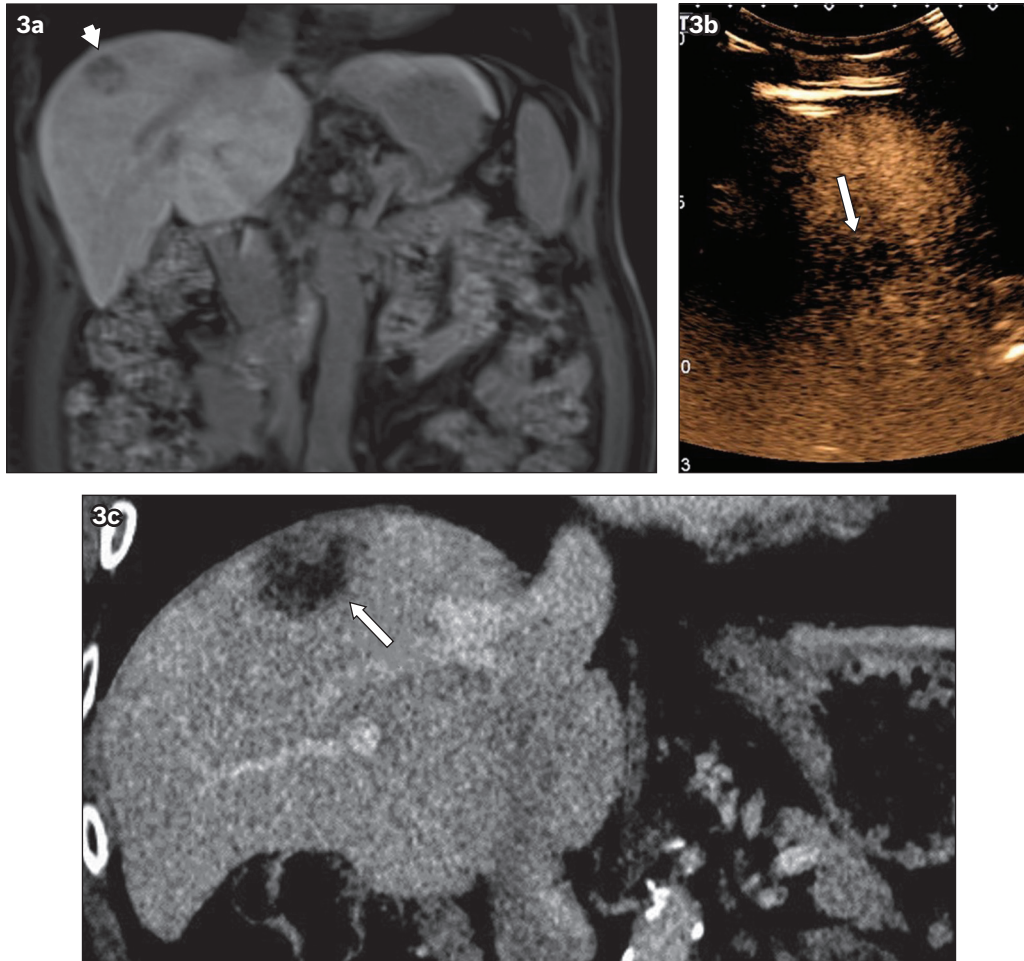


Fig. 3 (a) MR image of the liver shows a subphrenic Segment VIII tumour (arrowhead), which was (b) barely visualised on the pCEUS image (arrow) with a small intercostal acoustic window. Ablation was performed under US guidance. (c) Follow-up CT image after 12 months shows local tumour progression, with a solid enhancing focus noted at the superior aspect of the ablation zone (arrow). pCEUS: perfluorobutane-contrast-enhanced ultrasonography

administered intravenously, followed by 5 mL of normal saline flush. The operator then performed targeted sonography using the contrast-enhanced harmonic imaging mode at the recommended low mechanical index setting of 0.2, with a low-frequency convex probe operating at 2–5 MHz. US systems included the Philips Affiniti 50, Toshiba Aplio™ 500 and Esaote MyLab™Six. The RFA probe (or microwave antenna) was placed during the Kupffer phase about 10–15 minutes after injection (Fig. 2). CT localisation was used, with or without contrast, if the tumour was not detected following pCEUS.

Thermal ablations were performed under deep sedation or general anaesthesia. The Cool-tip™ (Covidien, Boulder, CO, USA) ablation system, using straight 17G ablation needles, was employed for RFA. The number of needles and duration of treatment were determined based on the tumour size and the desired ablation zone (i.e. at least 1 cm beyond the tumour borders). The Emprint™ (Covidien, Boulder, CO, USA) system was used for MWA, and ablation was performed for ten minutes. Tract ablation was performed during all probe removals. At the end of the treatment, non-contrast CT was performed to exclude immediate post-treatment complications (e.g. haematoma).

All patients were electively admitted for 1–2 days following treatment to allow a review of their inpatient clinical records.

Any minor or major complication, as defined by the Society of Interventional Radiology,⁽¹¹⁾ was noted, as well as any allergic reaction to contrast. Results of serial post-ablation liver function tests (LFTs), comprising total bilirubin, aspartate aminotransferase (AST), alanine aminotransferase (ALT), alkaline phosphatase and gamma-glutamyl transpeptidase tests, were also recorded.

Follow-up included clinic reviews at one and four weeks after discharge as well as a one-month post-treatment imaging study. Post-treatment imaging (i.e. multiphasic CT or liver-specific MR imaging) was performed at a median interval of 33 days. Based on the 2014 Society of Interventional Radiology-approved international consensus,⁽¹¹⁾ technical success or complete ablation was defined as complete coverage of the tumour by treatment ablation zone. Local tumour progression (LTP) was defined as detection of new tumour foci at the edge of the ablation zone (Fig. 3), while progression of the underlying disease was defined as new hepatic tumours or extrahepatic metastases. The aforementioned tumour data was retrieved from the electronic medical records for all patients until September 2017.

Tumour characteristics that potentially affected visibility on pCEUS, such as position, size and type, were compared between visible and non-visible lesions using Student's *t*-test for continuous variables and Pearson's chi-square test for categorical variables.

Table I. Baseline characteristics of patients who underwent pCEUS-guided tumour ablation (n = 35).

Characteristic	No. (%)
Gender	
Male	27 (77)
Female	8 (23)
Ethnicity	
Chinese	29 (83)
Indian	1 (3)
Malay	2 (6)
Burmese	3 (9)
Age* (yr)	65 (40–88)
Chronic liver disease/cirrhosis	31 (89)
Hepatitis B	11 (31)
Hepatitis C	5 (14)
Alcoholic cirrhosis	6 (17)
Cryptogenic cirrhosis/NASH	9 (26)
Child-Pugh score (n=31)	
A	24 (77)
B	7 (23)
Baseline albumin [†] (g/L)	42.0 (36.2–48.0)
Extrahepatic tumour with liver metastasis	4 (11)
Patients with ≥ 1 tumour treated per session	11 (31)
3 tumours	3 (9)
2 tumours	8 (23)

Data presented as *median (range) and †mean (range). NASH: non-alcoholic steatohepatitis

Using univariate logistic regression models, the odds ratio (OR) and 95% confidence interval (CI) of non-visibility on pCEUS for various lesion characteristics were calculated. Forward and backward stepwise selection methods were used to generate multivariate logistic regression models of non-visibility for lesion characteristics. A p-value < 0.05 was considered statistically significant. Statistical analysis was performed using Stata Statistical Software Release 14 (StataCorp, College Station, TX, USA).

RESULTS

The patient demographics and background clinical data of the 35 patients are summarised in Table I. The majority were Chinese male patients, with a median age of 65 years. Most treated tumours (89%) were primary HCCs, which were most commonly related to chronic viral hepatitis (31% and 14% of patients had hepatitis B and C, respectively). About one-third of patients (26%) had cryptogenic cirrhosis/nonalcoholic steatohepatitis, while 17% had cirrhosis attributed to chronic alcohol ingestion. 4 (11%) patients had hepatic metastases: colorectal adenocarcinoma in three patients (six lesions) and gastric adenocarcinoma in one patient (one lesion). Prior to treatment, patients were considered functionally fit with a pre-treatment ECOG (Eastern Cooperative Oncology Group) performance status⁽¹²⁾ score < 2 and good liver function, with 77% of patients who had chronic liver disease having a

Table II. Pre-treatment imaging characteristics of tumours (n = 48).

Characteristic	No. (%)
Tumour type	
Hepatocellular carcinoma	41 (85)
Metastasis	7 (15)
Tumour size* (maximal diameter in cm)	1.2 (0.7–3.0)
Pre-treatment imaging	
Multiphasic CT	29 (60)
Multiphasic CT + liver-specific MR imaging	8 (17)
Liver-specific MR imaging	10 (21)
Non-contrast MR imaging followed by pCEUS	1 (2)

*Data presented as median (range). CT: computed tomography; MR: magnetic resonance; pCEUS: perfluorobutane-contrast-enhanced ultrasonography

Table III. Variables associated with non-visualisation on pCEUS, assessed using multivariate regression models.

Variable	OR (95% CI)	p-value
Subdiaphragmatic location	13.7 (2.08–89.82)	0.005*
Deep/posterior location	6.64 (1.47–30.01)	0.008*
Child-Pugh Class B cirrhosis	6.88 (1.02–46.23)	0.003*
Size ≥ 1 cm	0.29 (0.07–1.11)	0.075
Liver segment		
I	9.52 (0.36–50.20)	0.177
II	0.73 (0.07–7.22)	0.786
III	0.38 (0.18–7.95)	0.535
IV	0.56 (0.06–5.37)	0.618
V	1.17 (0.25–5.36)	0.843
VI	1.00 (0.17–5.77)	1.000
VII	1.00 (0.17–5.77)	1.000
VIII	1.60 (0.25–10.07)	0.616
Classical features of HCC		
CT	1.12 (0.30–4.20)	0.867
MR imaging	0.25 (0.05–1.31)	0.100

*p < 0. CI: confidence interval; CT: computed tomography; HCC: hepatocellular carcinoma; MR: magnetic resonance; OR: odds ratio; pCEUS: perfluorobutane contrast-enhanced ultrasonography

Child-Pugh score of A.⁽¹³⁾ Post-treatment imaging data was not available for three patients who were subsequently managed at overseas centres. The remaining 32 patients had long-term follow-up data ranging from 12 to 28 months.

With regard to the imaging features of the tumours, except for one lesion that was 3 cm in diameter, the majority were ≤ 2 cm (Table II). On pCEUS, 36 (75%) out of 48 tumours were visualised. The 12 (25%) tumours not detected on pCEUS were targeted on either contrast-enhanced CT (n = 4, 8%) or non-contrast enhanced CT with anatomical correlation (n = 8, 17%).

Multivariate logistic regression models showed three variables to be statistically significant (p < 0.05) for predicting tumour non-visibility on pCEUS: (a) tumour in a subdiaphragmatic location; (b) tumour in a deep posterior location; and (c) the presence of Child-Pugh Class B cirrhosis (Table III).

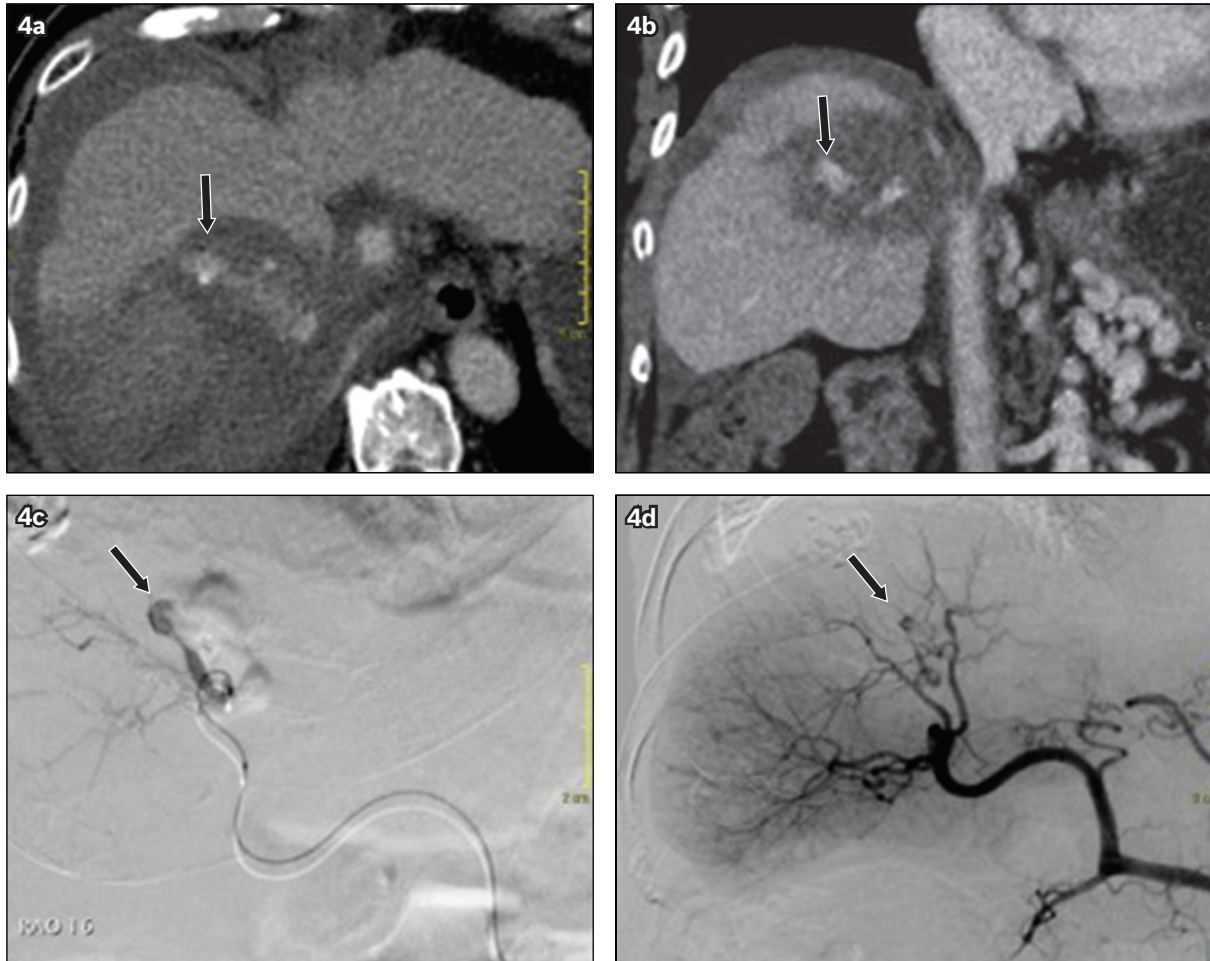


Fig. 4 (a) Axial and (b) coronal CT images of a patient who underwent ablation of a Segment VIII tumour a week earlier show perihepatic haematoma with active arterial bleed and a pseudoaneurysm (arrow) within the ablation zone. (c & d) Angiographic images show confirmation of the arterial pseudoaneurysm (arrow), which was subsequently embolised.

Based on the calculated ORs, several other variables may also have affected tumour visibility on pCEUS, although these were not statistically significant (Table III). Possible factors related to non-visualisation (i.e. OR > 1.00) include tumour location in Segment I or Segment VIII of the liver. On the other hand, factors that may predict tumour visibility (i.e. OR < 1.00) include tumour location in (a) Segment II, (b) Segment III or (c) Segment IV of the liver, (d) tumour size ≥ 1 cm and (e) the presence of classical MR imaging features of HCCs. Factors with ORs close to or equal to 1.00 probably do not affect tumour visibility on pCEUS.

Treatment outcomes and long-term follow-up data are shown in Table IV. One major complication of delayed post-ablation haemorrhage (occurring five days later) was observed, necessitating selective angioembolisation (Fig. 4). Minor complications (17%) included a case of small subcapsular haematoma that was managed expectantly and five patients with post-ablation pain that was relieved with oral analgesia. There was no reported US contrast allergy.

LFTs were usually performed a week after treatment, although nine patients had LFTs done just prior to discharge. The most consistently elevated liver enzymes were AST and ALT, with the largest rise being recorded during the first two post-treatment days, up to around 13- and 15-fold for AST and ALT, respectively. LFTs returned to normal for most patients within a week and took up

Table IV. Treatment outcome and long-term follow-up data.

Parameter	No. (%)
Complete ablation (n = 46)	41 (89)
Complications (n = 35)	
Major	
<i>Significant haemorrhage requiring angioembolisation</i>	1 (3)
Minor	
<i>Small subcapsular haematoma</i>	1 (3)
<i>Post-ablation pain</i>	5 (14)
Liver function derangement (n = 34)	
Returned to baseline within 1 wk*	29 (85)
Long-term survival	
Local tumour progression (n = 46)	8 (17)
Median time to local tumour progression (mth)	14
New tumours (n = 33)	8 (24)
End-stage progression of underlying disease (n = 33)	3 (9)

Percentages were calculated based on value of n.

to about five months for the remaining 14%. None of the patients had persistent or progressively worsening LFTs.

34 patients had one-month post-ablation imaging for 46 treated tumours. The overall complete ablation rate was

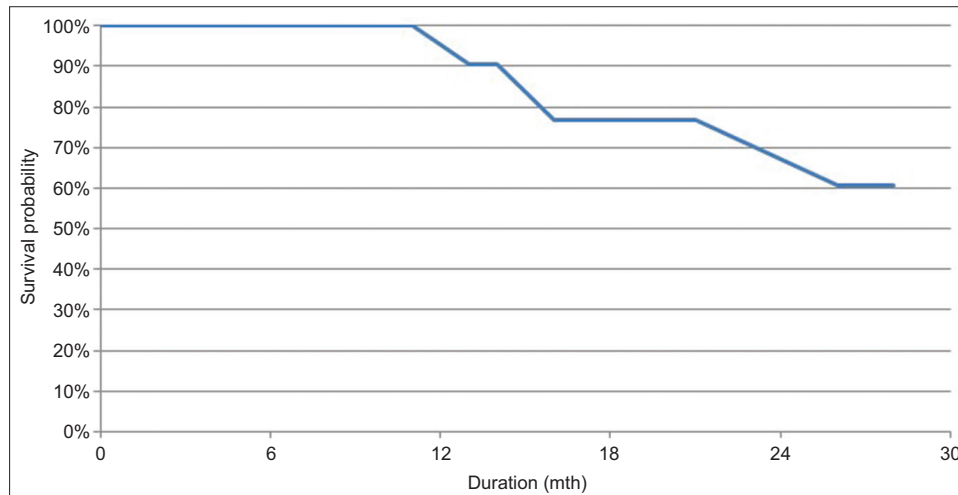


Fig. 5 Kaplan-Meier plot shows local tumour progression-free survival.

89% (n = 41), although 8 (20%) of these were not visualised on pCEUS and required additional CT fluoroscopy during treatment. Of the five residual tumours, one underwent successful repeat ablation at the one-month interval. Another incompletely ablated lesion (a HCC), which had an indeterminate enhancing residual component on subsequent CT images, demonstrated long-term size stability over 18 months and was deemed non-malignant following serial multidisciplinary discussions. Repeat treatment was not performed for the remaining three tumours (from two separate patients) as per the patients' wishes.

New hepatic tumours developed in 24% of patients, while another 9% developed end-stage progression of disease (either extrahepatic metastases or clinical liver failure), rendering them unsuitable for further treatment. The LTP rate was 17%, with the majority occurring after 12 months. The survival probability, defined as the LTP-free interval, was estimated using the Kaplan-Meier method (Fig. 5).

DISCUSSION

Detection rates of small hepatic tumours (≤ 3 cm) on targeted greyscale US were reported to range from about 60% to 80%, reducing to about 30% when the tumour size was ≤ 1 cm.^(14,15) Several studies, of which the highest level of evidence was Level 2b,⁽¹⁶⁾ support the use of contrast-enhanced US for hepatic tumour ablation. We opine that pCEUS is superior owing to its additional Kupffer phase.

pCEUS, which is already prevalent in South Korea and Japan as both a diagnostic and an interventional adjunct, has only recently been introduced in Singapore. Current evidence regarding its practical benefits in the interventional suite has not been validated outside the Japanese and Korean populations. However, the superior detection rate of pCEUS has been established, especially in the context of hepatic metastases,^(17,18) with its sensitivity doubling when added to conventional greyscale US. Masuzaki et al reported a close to 10% increased detection rate of small hepatic tumours with pCEUS.⁽¹⁵⁾ While our detection rate of 75% for tumours that were imperceptible on greyscale US was relatively high, it is still lower than that reported by Japanese and Korean authors, who reported a detection rate of up to 90%.^(19,20)

This may be attributed to user experience or population differences.

Our technical success rate of 89% based on a single ablation attempt (i.e. the primary success rate) compared favourably with the local historical data of 87.3% (for tumours smaller than 3.0 cm),⁽²¹⁾ as well as with international reports of $\geq 80\%$ for liver tumour RFA.^(22,23) Kelogrigoris et al reported a similar rate of 87.3% when CT fluoroscopy was employed.⁽²⁴⁾ In Dohmen et al's 2012 retrospective analysis,⁽²⁵⁾ which also evaluated pCEUS, technical success was assessed for multiphasic CT performed 3–5 days after treatment. The study introduced the term 'radicality', graded from R0 to R3 depending on the degree of tumour coverage by the ablation zone, with R2 and R3 lesions having complete coverage. Based on this definition, Dohmen et al had a 'technical success' rate of 67.6% (i.e. comprising R2 and R3 lesions). Although our results are not directly comparable owing to the differences between the assessment methods, we found it reasonable to conclude that our treatment outcomes were well within the standard for this sonographically occult group of tumours.

Unlike other cross-sectional imaging modalities that run on established protocols and defined scan planes, US is a dynamic tool that produces highly variable images depending on a multitude of factors. Even with an experienced operator, several patient-disease factors can limit the study. Lee et al⁽¹⁴⁾ found that the two most significant factors were tumour size (diameter ≤ 1 cm) and a subdiaphragmatic location. pCEUS does not entirely negate these obstacles. In our series, a challenging tumour location (either in a subdiaphragmatic or deep posterior location) and the presence of more advanced cirrhosis (i.e. Child-Pugh Class B cirrhosis) were statistically significant independent factors contributing to non-visualisation on PCEUS. The subdiaphragmatic position is a technically difficult location to image because of sonographic scattering produced by gas within the lungs. Further, it often requires intercostal positioning of the US probe, especially with elderly patients who are unable to fully inspire or hold their breaths, which inadvertently leads to a poor acoustic window (Fig. 6). One safe and effective problem-solving technique that has been described is the production of artificial

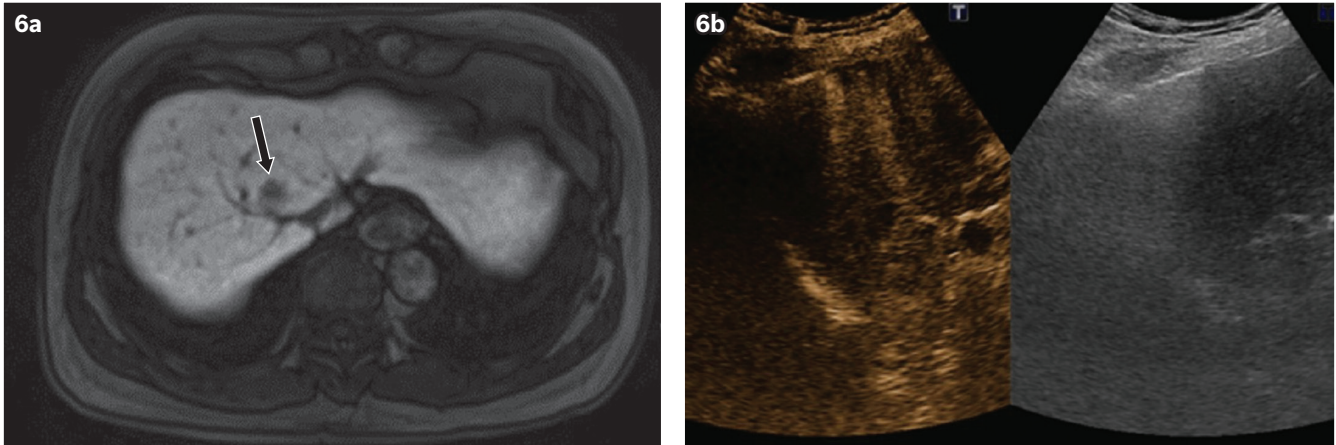


Fig. 6 (a) Liver-specific MR image shows a Segment VIII tumour visualised as a hypointense 'defect' on the hepatobiliary phase (arrow). (b) Corresponding pCEUS image shows a significant amount of posterior acoustic shadowing and lack of a satisfactory acoustic window, thereby severely limiting lesion detection. pCEUS: perfluorobutane contrast-enhanced ultrasonography

right pleural effusion.⁽²⁶⁾ After treatment, the pleural effusion is expected to resolve within a week.

Lesion localisation is difficult in cirrhotic livers because of background nodular heterogeneity and the concomitant presence of other non-malignant (regenerative/dysplastic) nodules. Further, liver impairment may reduce the ability of Kupffer cells to phagocytose, therefore reducing the contrast between the tumour and the adjacent parenchyma on the delayed Kupffer phase. Tanimoto et al⁽²⁷⁾ provided support for this hypothesis with MR imaging by employing superparamagnetic iron oxide, another contrast agent that is phagocytosed by Kupffer cells.

As perfluorobutane microbubbles are stabilised by hydrogenated egg phosphatidylserine membranes,⁽²⁸⁾ pCEUS is contraindicated in patients with known egg allergies. None of the treated patients in this study had a known history of egg allergy or developed any allergic reaction following treatment. Overall, perfluorobutane-based contrast has an established safety profile, with reported drug reactions such as diarrhoea being mild and self-limiting,^(29,30) while severe allergic reactions have yet to be reported.

Image-guided thermal ablation, especially RFA, has long been established as being relatively low risk. A 2014 systemic review⁽³¹⁾ reported major complication rates of 4.1% and 4.6%, with mortality rates of 0.15% and 0.23% for RFA and MWA, respectively. Among the major complications, postprocedural haemorrhage requiring blood transfusion was the most common. In this regard, the 3% major complication rate (in one patient) and 0% mortality rate in this study fall within the acceptable risk limits.

In conclusion, pCEUS has a role in US-guided ablation of small liver tumours. The ability for real-time scanning with an extended targeting window makes it a powerful adjunct when targeting tumours that are poorly visualised on non-enhanced greyscale US. Our study suggests that 75% of tumours that are otherwise sonographically occult may be treated with pCEUS without compromising treatment outcomes. Our high technical success rate of 89% is comparable to reported data pertaining to both US and CT-guided techniques. Further, compared to CT

fluoroscopy, pCEUS offers improved procedure time and freedom from ionising radiation for both the patient and the operator.

REFERENCES

- Weis S, Franke A, Mössner J, Jakobsen JC, Schoppmeyer K. Radiofrequency (thermal) ablation versus no intervention or other interventions for hepatocellular carcinoma. *Cochrane Database Syst Rev* 2013; (12):CD003046.
- Lau WY, Lai EC. The current role of radiofrequency ablation in the management of hepatocellular carcinoma: a systematic review. *Ann Surg* 2009; 249:20-5.
- Wells SA, Hinshaw JL, Lubner MG, et al. Liver ablation: best practice. *Radiol Clin North Am* 2015; 53:933-71.
- Xu JF, Liu HY, Shi Y, Wei ZH, Wu Y. Evaluation of hepatocellular carcinoma by contrast-enhanced sonography: correlation with pathologic differentiation. *J Ultrasound Med* 2011; 30:625-33.
- Yanagisawa K, Moriyasu F, Miyahara T, Yuki M, Iijima H. Phagocytosis of ultrasound contrast agent microbubbles by Kupffer cells. *Ultrasound Med Biol* 2007; 33:318-25.
- Nakano H, Ishida Y, Hatakeyama T, et al. Contrast-enhanced intraoperative ultrasonography equipped with late Kupffer-phase image obtained by sonazoid in patients with colorectal liver metastases. *World J Gastroenterol* 2008; 14:3207-11.
- Korenaga K, Korenaga M, Furukawa M, Yamasaki T, Sakaida I. Usefulness of sonazoid contrast-enhanced ultrasonography for hepatocellular carcinoma: comparison with pathological diagnosis and superparamagnetic iron oxide magnetic resonance images. *J Gastroenterol* 2009; 44:733-41.
- Omata M, Cheng AL, Kokudo N, et al. Asia-Pacific clinical practice guidelines on the management of hepatocellular carcinoma: a 2017 update. *Hepatol Int* 2017; 11:317-70.
- Rhim H, Lee MH, Kim YS, et al. Planning sonography to assess the feasibility of percutaneous radiofrequency ablation of hepatocellular carcinomas. *AJR Am J Roentgenol* 2008; 190:1324-30.
- Chung YE, Kim KW. Contrast-enhanced ultrasonography: advance and current status in abdominal imaging. *Ultrasonography* 2015; 34:3-18.
- Ahmed M, Solbiati L, Brace CL, et al. Image-guided tumor ablation: standardization of terminology and reporting criteria--a 10-year update. *Radiology* 2014; 273:241-60.
- Oken MM, Creech RH, Tormey DC, et al. Toxicity and response criteria of the Eastern Cooperative Oncology Group. *Am J Clin Oncol* 1982; 5:649-55.
- Child CG, Turcotte JG. Surgery and portal hypertension. *Major Probl Clin Surg* 1964; 1:1-85.
- Lee MW, Kim YJ, Park HS, et al. Targeted sonography for small hepatocellular carcinoma discovered by CT or MRI: factors affecting sonographic detection. *AJR Am J Roentgenol* 2010; 194:W396-400.
- Masuzaki R, Shiina S, Tateishi R, et al. Utility of contrast-enhanced ultrasonography with sonazoid in radiofrequency ablation for hepatocellular carcinoma. *J Gastroenterol Hepatol* 2011; 26:759-64.
- Minami Y, Kudo M. Review of dynamic contrast-enhanced ultrasound guidance in ablation therapy for hepatocellular carcinoma. *World J Gastroenterol* 2011; 17:4952-9.
- Sugimoto K, Shiraishi J, Moriyasu F, Saito K, Doi K. Improved detection of hepatic metastases with contrast-enhanced low mechanical-index pulse inversion ultrasonography during the liver-specific phase of sonazoid: observer

- performance study with JAFROC analysis. *Acad Radiol* 2009; 16:798-809.
18. Correas JM, Low G, Needleman L, et al. Contrast enhanced ultrasound in the detection of liver metastases: a prospective multi-centre dose testing study using a perfluorobutane microbubble contrast agent (NC100100). *Eur Radiol* 2011; 21:1739-46.
 19. Numata K, Morimoto M, Ogura T, et al. Ablation therapy guided by contrast-enhanced sonography with sonazoid for hepatocellular carcinoma lesions not detected by conventional sonography. *J Ultrasound Med* 2008; 27:395-406.
 20. Min JH, Lim HK, Lim S, et al. Radiofrequency ablation of very-early-stage hepatocellular carcinoma inconspicuous on fusion imaging with B-mode US: value of fusion imaging with contrast-enhanced US. *Clin Mol Hepatol* 2014; 20:61-70.
 21. Low SC, Lo RH, Lau TN, et al. Image-guided radiofrequency ablation of liver malignancies: experience at Singapore General Hospital. *Ann Acad Med Singapore* 2006; 35:851-7.
 22. Rossi S, Di Stasi M, Buscarini E, et al. Percutaneous RF interstitial thermal ablation in the treatment of hepatic cancer. *AJR Am J Roentgenol* 1996; 167:759-68.
 23. Livraghi T, Goldberg SN, Lazzaroni S, et al. Hepatocellular carcinoma: radiofrequency ablation of medium and large lesions. *Radiology* 2000; 214:761-8.
 24. Kelogrigoris M, Laspas F, Kyrkou K, et al. Percutaneous radiofrequency ablation for malignant liver tumours in challenging locations. *J Med Imaging Radiat Oncol* 2012; 56:48-54.
 25. Dohmen T, Kataoka E, Yamada I, et al. Efficacy of contrast-enhanced ultrasonography in radiofrequency ablation for hepatocellular carcinoma. *Intern Med* 2012; 51:1-7.
 26. Wang G, Sun Y, Cong L, Jing X, Yu J. Artificial pleural effusion in percutaneous microwave ablation of hepatic tumors near the diaphragm under the guidance of ultrasound. *Int J Clin Exp Med* 2015; 8:16765-71.
 27. Tanimoto A, Yuasa Y, Shinmoto H, et al. Superparamagnetic iron oxide-mediated hepatic signal intensity change in patients with and without cirrhosis: pulse sequence effects and Kupffer cell function. *Radiology* 2002; 222:661-6.
 28. Sontum PC. Physicochemical characteristics of sonazoid, a new contrast agent for ultrasound imaging. *Ultrasound Med Biol* 2008; 34:824-33.
 29. Moriyasu F, Itoh K. Efficacy of perflubutane microbubble-enhanced ultrasound in the characterization and detection of focal liver lesions: phase 3 multicenter clinical trial. *AJR Am J Roentgenol* 2009; 193:86-95.
 30. Numata K, Luo W, Morimoto M, et al. Clinical usefulness of contrast-enhanced three-dimensional ultrasound imaging with sonazoid for hepatic tumor lesions. *World J Radiol* 2010; 2:68-82.
 31. Lahat E, Eshkenazy R, Zendel A, et al. Complications after percutaneous ablation of liver tumors: a systematic review. *Hepatobiliary Surg Nutr* 2014; 3:317-23.